Available online at www.sciencedirect.com
SCIENCE DIRECT
Polymer 47 (2006) 5946–5951
polymer
www.elsevier.com/locate/polymer

Incoherent neutron scattering study on the local dynamics in polystyrene and poly(vinyl methyl ether) blends

Hiroyuki Takeno [a,*], Satoshi Koizumi [b]

[a] Department of Biological and Chemical Engineering, Faculty of Engineering, Gunma Univeristy, 1-5-1 Tenjin-cho, Kiryu, Gunma 376-8515, Japan
[b] Research Group of Soft-Matter and Neutron Scattering, Advanced Science Research Center, Japan Atomic Energy Research Institute, Tokai, Ibaraki-ken 319-1195, Japan

Received 5 November 2005; received in revised form 11 June 2006; accepted 14 June 2006
Available online 7 July 2006

Abstract

Neutron scattering study using the fixed elastic window technique is performed to investigate the effect of blending on the local dynamics of each component for polystyrene and poly(vinyl methyl ether) blends. The non-Gaussian scattering behavior observed above a certain temperature for the PVME component can be well explained by considering the rotational motions of methyl groups around O–CH_3 axis. The mean-square displacements of the vibrational motions were approximately proportional to absolute temperature below the glass transition temperature, which is a signature of harmonic oscillations, and were hardly affected by blending PS. On the other hand, the mean-square displacement of the PS component in the blend was almost the same as that of pure PS, while the non-Gaussian parameter for the former was much larger in comparison with that of the latter. Blending with PVME leads to a large increase in the dynamical heterogeneity for the PS component.

Keywords: Neutron scattering; Local dynamics; Polymer blend

1. Introduction

The molecular motions in condensed matters have been investigated in great deal using various spectroscopic techniques such as neutron scattering, light scattering, dielectric spectroscopy, nuclear magnetic resonance (NMR), etc. The neutron scattering measurements have an advantage that they can provide information about the spatial extent of molecular motions on a microscopic scale as well as the time dependence [1]. Local dynamics such as vibrational motions or rotational motions of methyl groups is active even in the glassy state. The fixed elastic window technique has been used to investigate the local dynamics of polymers [2–4]. In this technique, we observe the scattering at a fixed elastic window at $\omega \approx 0$, which depends upon the energy resolution of the spectrometer used. The scattering intensity observed in the window may be represented as follows:

$$I_{el}(q, \omega \approx 0) = \int_{-\Delta\omega}^{\Delta\omega} I(q, \omega) d\omega, \quad (1)$$

where $\Delta\omega$ and q represent the half-width half maximum (hwhm) of the instrumental resolution function and the magnitude of wave vector expressed by $q = (4\pi/\lambda)\sin(\theta/2)$, respectively. λ and θ are the neutron wavelength and scattering angle, respectively. At low temperatures, purely elastic scattering and quasielastic scattering lie within the elastic window. When the time scale of a molecular motion becomes comparable with the energy resolution of the spectrometer with increasing temperature, the quasielastic scattering broadens, which causes reduction of $I_{el}(q, \omega \approx 0)$. Thus, we can obtain information on the local dynamics from $I_{el}(q, \omega \approx 0)$.

In this study, in order to investigate the effects of blending on the local dynamics in polystyrene and poly(vinyl methyl

* Corresponding author. Tel.: +81 277 30 1476; fax: +81 277 30 1409.
E-mail address: takeno@bce.gunma-u.ac.jp (H. Takeno).

0032-3861/$ - see front matter © 2006 Elsevier Ltd. All rights reserved.
doi:10.1016/j.polymer.2006.06.028

ether) blends, we performed the neutron scattering measurements using the fixed elastic window technique for four samples; pure polystyrene (PS), pure poly(vinyl methyl ether) (PVME), a blend of deuterated PS (dPS) and PVME, a blend of protonated PS and PVME. In neutron scattering measurements, as the incoherent scattering length of hydrogen atoms is very large compared to that of other atoms or coherent scattering length of any atoms, we expect to pursue molecular motions of the systems through incoherent scattering of hydrogen atoms e.g., the scattering for the dPS/PVME blend is expected to come from the incoherent contribution of the component of PVME. Here we deal with the local dynamics below glass transition temperature T_g and shall discuss the influence of blending on it.

2. Experimental

2.1. Sample characterization and preparation

PVME and PS used in this study were obtained from Aldrich Co. The former was fractionated by using toluene as a good solvent and hexane as a poor one. PVME and PS have the number-averaged molecular weight M_n of 2.1×10^4 and 6.0×10^4, respectively, and heterogeneity index for molecular weight distribution M_w/M_n of 1.92 and 1.03, respectively. The dPS with M_n of 4.8×10^4 and M_w/M_n of 1.05 was obtained from Polymer Source Co. We prepared blends of PS with PVME and dPS with PVME having composition of 50/50 wt/wt %. Both blends were dissolved in toluene. After the solution was cast into films by evaporating the solvent at room temperature, the films obtained were dried under vacuum oven for 3 days at ca. 80–100 °C for pure PVME and the blends, and at ca. 150 °C for pure PS in order to perfectly remove the solvent.

2.2. Neutron scattering measurements

Neutron scattering experiments were carried out by use of a cold triple-axis spectrometer (LTAS) at the Japan Atomic Energy Research Institute in Tokai in Japan. Instrumental resolution was investigated by performing an energy scan at constant q for vanadium. Such experiments were performed at six qs in the q range from 0.2 to 2.4 Å^{-1}. The instrumental resolution can be represented by Gaussian function with half-width half maximum (hwhm) between 86 and 93 μeV, which is almost independent of q. We measured the data in the elastic window fixed at $\omega \approx 0$ for four samples: (i) PVME; (ii) PS; (iii) dPS/PVME blend; (iv) PS/PVME blend.

3. Results and discussion

3.1. Incoherent scattering analysis

Fig. 1 shows the scattering profiles of pure PVME at various temperatures. They have a small peak at ca. $q = 1.2$ Å^{-1}, which is considered to be due to contribution of the coherent scattering. We try to remove it in order to perform the incoherent scattering analysis. We tried to eliminate the coherent effects by dividing the scattering at a given temperature $I(q, \omega \approx 0, T)$ by the scattering at the lowest temperature $I(q, \omega \approx 0, T_{min})$ in the similar manner as many researchers carried out [5]. The logarithm of the divided scattering intensity obtained thus, $\ln[I(q, \omega \approx 0, T)/I(q, \omega \approx 0, T_{min})]$ decreases monotonously with increase of q for all the systems (see Fig. 2).

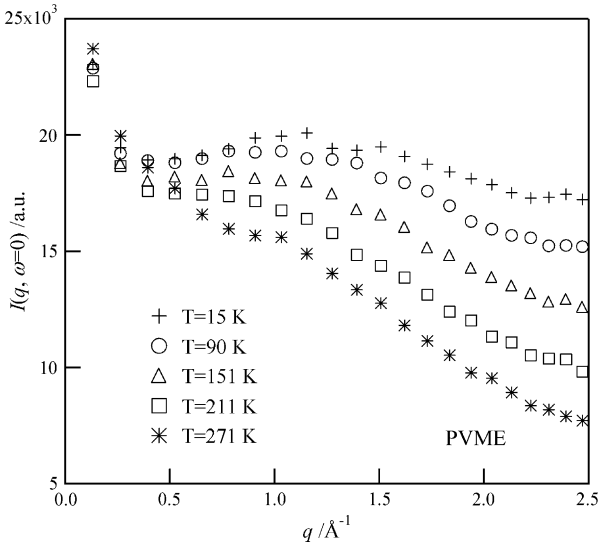

Fig. 1. Scattering profiles for PVME at various temperatures.

Incoherent elastic scattering through vibrational motions can be well described by Debye–Waller factor,

$$I_{el}(q, \omega = 0) = I_0 \exp[-\langle u^2 \rangle q^2], \tag{2}$$

where I_0 and $\langle u^2 \rangle$ are constants which depend upon experimental condition and the mean-square displacement, respectively. However, as a matter of fact, it has been often shown that the logarithm of the elastic incoherent scattering for many glass formers does not show a linear dependence against q^2, but has a curvature [6]. In such cases, the expansion up to q^4 can well represent the scattering behavior [7]

$$I(q, \omega = 0) = I_0 \exp\left[-\langle u^2 \rangle q^2 + \frac{1}{2} A \langle u^2 \rangle^2 q^4\right], \tag{3}$$

where A is a non-Gaussian parameter. Such deviation from the Gaussian behavior has been explained by distribution of the displacements of the protons or anharmonicity of potentials [8].

If we assume that ratio of the coherent scattering at T, $I_{coh}(q, \omega = 0, T)$ to that at T_{min}, $I_{coh}(q, \omega = 0, T_{min})$ is equal to that of incoherent scattering $I_{inc}(q, \omega = 0, T)/I_{inc}(q, \omega = 0, T_{min})$, then the following equation from Eq. (3) is obtained.

$$\ln[I(q, \omega = 0, T)/I(q, \omega = 0, T_{min})] = -\left(\langle u^2 \rangle_T - \langle u^2 \rangle_{T_{min}}\right) q^2 + \frac{1}{2}\left(A_T \langle u^2 \rangle_T^2 - A_{T_{min}} \langle u^2 \rangle_{T_{min}}^2\right) q^4. \tag{4}$$

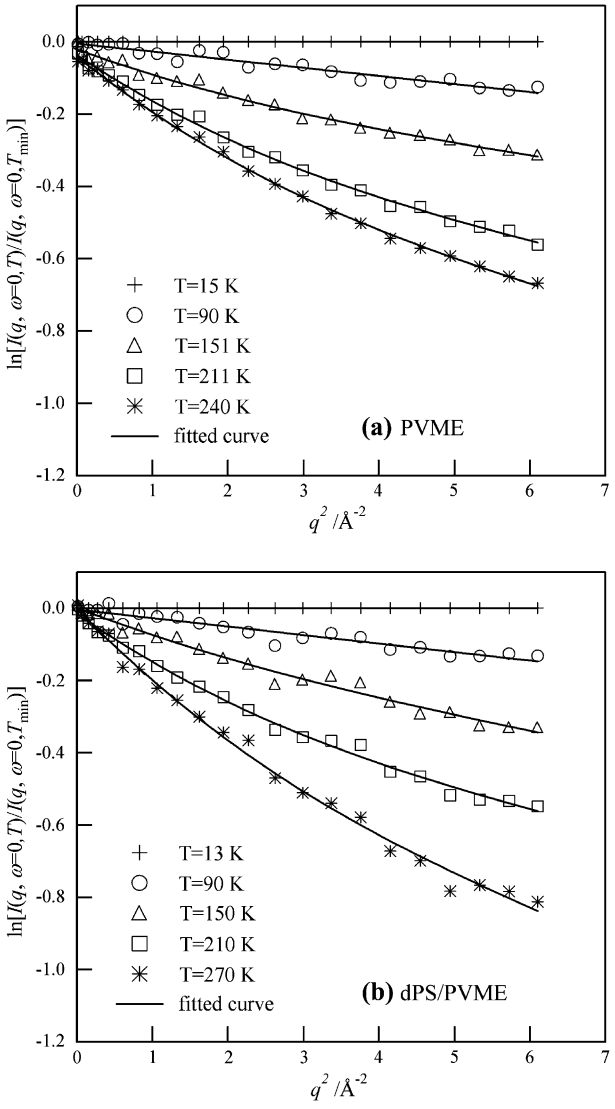

Fig. 2. Logarithm of scattering intensity divided by that at the lowest temperature (ca. 15 K) against q^2 for (a) PVME and (b) dPS/PVME blend at various temperatures.

Subscripts T and $T_{\min}$ represent the measured temperatures and the lowest temperature, respectively.

In Fig. 2, we present the plot of $\ln[I(q,\omega=0,T)/I(q,\omega=0,T_{\min})]$ against q^2 for pure PVME (a) and dPS/PVME blend (b) at various temperatures. The plots show a linear relation at low temperatures i.e., Gaussian behavior, while they have a curvature at high temperatures i.e., non-Gaussian behavior. Also, we show temperature dependence of the divided intensity $I(q,\omega=0,T)/I(q,\omega=0,T_{\min})$ at different qs for pure PVME in Fig. 3. The temperature dependence can be divided into two regions: $I(q,\omega=0,T)/I(q,\omega=0,T_{\min})$ at a given q linearly decreases with the increase of temperature at temperatures less than 90 K (region I), while it deviates downwards from the linearity at temperatures higher than it (region II). This behavior is consistent with the results from the quasielastic neutron scattering measurements by other researchers [9,10]. When we look at the scattering profiles in

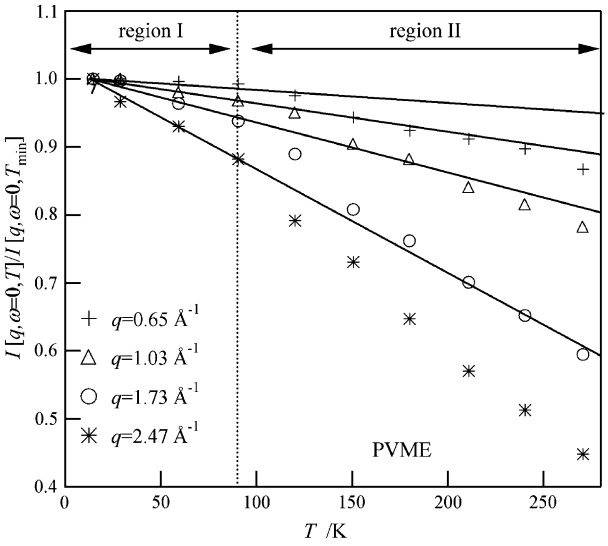

Fig. 3. Temperature dependence of the divided intensity for PVME at different q values.

Fig. 2, we see that the scattering behavior shows the Gaussian type in region I, while it does the non-Gaussian type in region II. The same plots for the other three systems show similar trend, although they are not seen here.

3.2. Local dynamics of PVME component

First, let us analyze the local dynamics for the PVME component. As mentioned above, $\ln[I_T(q,\omega=0)/I_{T_{\min}}(q,\omega=0)]$ has a linear relation against q^2 in region I i.e., A_T in Eq. (4) is zero, while it has a concave curvature in region II i.e., A_T has a positive value which is not zero. Therefore, in region I by letting $A_{T_{\min}}=0$ and $A_T=0$, we fitted Eq. (4) to the data of $\ln[I_T(q,\omega=0)/I_{T_{\min}}(q,\omega=0)]$ at each temperature with adjustable parameters of $(\langle u^2\rangle_T-\langle u^2\rangle_{T_{\min}})$ and q-independent background which may be caused by fast motions which are not taken into consideration in Eq. (4) and/or contribution of some residual instrumental background. Since the $(\langle u^2\rangle_T-\langle u^2\rangle_{T_{\min}})$ obtained thus showed a linear temperature dependence, we determined $\langle u^2\rangle_T$ and $\langle u^2\rangle_{T_{\min}}$ from the relation of $\langle u^2\rangle_T=aT$ (a is a constant) as expected in harmonic vibration.

The non-Gaussian behavior in region II may be due to the rotation of the methyl group about O–CH_3 axis as shown from quasielastic measurements by other researchers [9–11], where they consider the jump among three equivalent sites equally space on a circle. Here, we also consider the similar rotational motions of methyl groups around O–CH_3 axis for the scattering behavior in the region II i.e., the non-Gaussian behavior in the region II is caused by broadening of quasielastic scattering arising from rotational motions of the methyl groups. If we assume there is no correlation of vibrational and rotational motions, the incoherent scattering intensity is given as follows

$$I(q,\omega)=I_0\exp\left(-\langle u^2\rangle q^2\right)\left[\frac{1}{2}+\frac{1}{2}S^{\mathrm{rot}}(q,\omega)\right], \tag{5}$$

where I_0 is a constant which depends on the experimental condition and $S^{\mathrm{rot}}(q,\omega)$ is a dynamical structure factor arising from the rotational motions [9–11]. The former 1/2 and the latter 1/2 in the parenthesis represent the fraction of number of hydrogen atoms in the main chain and that of side groups (methyl groups) among monomer unit, respectively. $S^{\mathrm{rot}}(q,\omega)$ consists of two contributions of the pure elastic component and the quasielastic component [9–11]. Besides the elastic component in the strict meaning, the quasielastic part of $S^{\mathrm{rot}}(q,\omega)$ also contributes to the scattering observed at the fixed elastic window which depends upon the energy resolution as shown in Eq. (1). Namely, the quasielastic component less than the instrumental energy resolution (hwhm = 86 – 93 μeV), to be more accurate, that of $S^{\mathrm{rot}}(q,\omega)$ convoluted with the instrumental energy resolution less than it can be observed in the elastic window scans. Thus, the observed elastic scattering normalized by that at the lowest temperature is given by

$$\ln[I(q,\omega=0,T)/I(q,\omega=0,T_{\min})] = -\left(\langle u^2\rangle_T - \langle u^2\rangle_{T_{\min}}\right)q^2 + \ln\left[\frac{1}{2}+\frac{1}{2}S^{\mathrm{rot}}(q,\omega\approx 0)\right] \quad (6)$$

with

$$S^{\mathrm{rot}}(q,\omega\approx 0) = A(q) + \{1-A(q)\}\alpha, \quad (7)$$

where $A(q)$ is given by the following form

$$A(q) = \frac{1+2j_0(qr_{\mathrm{H-H}})}{3} \quad (8)$$

and α is a fraction of the quasielastic component in the range within the full-width half maximum (fwhm) of the instrumental resolution function. In the above equation, j_0 is the zeroth-order Bessel function and $r_{\mathrm{H-H}}$ is the hydrogen–hydrogen distance in the methyl groups. Here α is assumed to be independent of q, as shown by other researchers [9].

For data in region II, we carried out the fitting procedure with Eqs. (6) and (7) by adopting $\langle u^2\rangle_T$, α, q-independent background as adjustable parameters. In Fig. 2 we show the comparison between the data and the fitted curves for pure PVME (a) and dPS/PVME blend (b). Fitted curves describe the data well. We precluded the data at 271 K for PVME from the fitting procedure, because the temperature is larger than the glass transition temperature [12] and the factors other than rotational motions of methyl groups may affect the scattering behavior. The temperature dependence of $\langle u^2\rangle_T$ and α obtained in this fitting procedure is shown in Fig. 4. For comparison we also show $\langle u^2\rangle_T$ estimated by fitting of Eq. (4) in region I, where all the rotational motions of methyl group lie within the instrumental resolution of our apparatus. As shown in Fig. 4(a), $\langle u^2\rangle_T$ obtained from the fit with Eqs. (6) and (7) is found to be almost proportional to absolute temperature for both pure PVME and dPS/PVME blend in the glassy state. This behavior suggests that the vibrational motions are approximately harmonic until the temperature approaches T_g. Moreover, $\langle u^2\rangle_T$ and α for dPS/PVME blend show almost the same values as those of pure PVME. Thus, it is shown that the motions of PVME are almost not affected by blending.

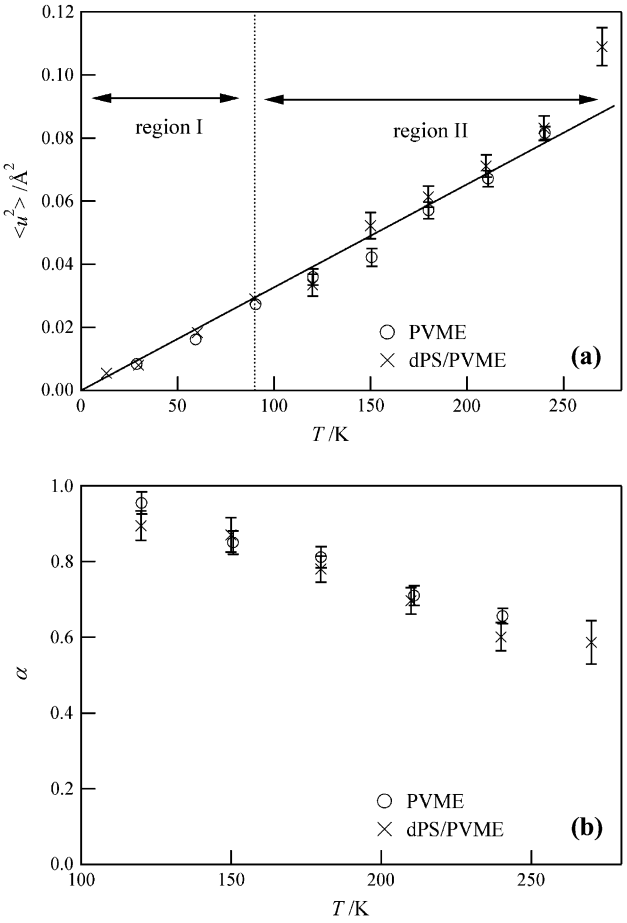

Fig. 4. Temperature dependence of (a) mean-square displacement and (b) α for PVME and dPS/PVME blend.

3.3. Estimation of the mean-square displacement and non-Gaussian parameter of the PS component

Next, let us analyze the scattering data for pure PS and PS/PVME blend. For pure PS, in region I we estimated the mean-square displacement in the same manner as that of PVME. In region II the fit to data were performed by considering $\langle u^2\rangle_T$, A_T and q-independent background as adjustable parameters in Eq. (4), where we used the value of $\langle u^2\rangle_{T_{\min}}$ obtained in region I and $A_{T_{\min}} = 0$.

On the other hand, in the case of PS/PVME blend, since both components include hydrogen atoms which are unique in having very large incoherent neutron scattering cross section, the observed scattering involves the contribution of scattering from both components. Accordingly, we carried out the analysis by assuming additivity of contribution of the PS component (Eq. (4)) and that of the PVME component (Eq. (6)) as follows.

$$\ln\left[\frac{I(q,\omega=0,T)}{I(q,\omega=0,T_{\min})}\right]=\ln\left\{\frac{C_1\exp\left[-\langle u^2\rangle_{1,T}q^2+\frac{1}{2}A_{1,T}\langle u^2\rangle_{1,T}^2q^4\right]+C_2\exp\left[-\langle u^2\rangle_{2,T}q^2\right]\left\{\frac{1}{2}+\frac{1}{2}S^{\mathrm{rot}}(q,\omega)\right\}}{C_1\exp\left[-\langle u^2\rangle_{1,T_{\min}}q^2\right]+C_2\exp\left[-\langle u^2\rangle_{2,T_{\min}}q^2\right]}\right\},\tag{9}$$

where subscripts 1 and 2 represent PS component and PVME component, respectively. Since there are too many adjustable parameters in the fitting to the data with Eq. (9), we fixed the parameters of the PVME component by using those estimated for dPS/PVME blend. Then we assumed the isotope effects are negligible. We estimated $\langle u^2\rangle_T$ and A_T for the PS component in the blend by the best fit of Eq. (9) to the data, where C_1/C_2 corresponds to the ratio of the number density of hydrogen atoms for component 1 to that of component 2. Fitted curves are in good agreement with the data as shown in Fig. 5. The $\langle u^2\rangle_T$ and A_T of the PS component in the blend are compared with those of pure PS in Fig. 6. Similar to PVME, the temperature dependence of their $\langle u^2\rangle_T$s can be separated into two regions. Namely, $\langle u^2\rangle_T$ is proportional to absolute temperature until ca. 150 K, while beyond the temperature it deviates upwards from the linearity. Furthermore, $\langle u^2\rangle_T$ of the PS component in PS/PVME blend has almost the same values as that of pure PS in the both regions, though they scatter a little. On the other hand, A_T of the PS component in PS/PVME blend is shown to decrease with increase of temperature. Moreover, it is found to be quite large in comparison with that of pure PS. Even if we took the error of the parameters of the PVME component, we can conclude that the non-Gaussian parameter of the PS component for the blend is significantly larger than that of pure PS.

According to Zorn [8], the positive value of A_T is caused by dynamical heterogeneity arising from the environmental difference around hydrogen atoms. The increase of the dynamical heterogeneity in the blend may take place especially due to the motions of phenyl groups. It has been reported by Fisher et al. that blending of polycarbonate of bisphenol A, which has phenyl groups in the chemical structure, with low molecular weight substance leads to a drastic increase of the width of distribution of correlation frequencies for the flipping motions of phenyl groups obtained by means of ^{2}H-NMR [13]. In the case of this blend, the phenyl groups in PS are bulky, while the methyl ether groups in PVME are small. Hence, we guess that the latter goes into interstices produced by the former to some degree, which affects the local dynamics of PS. The character of this blend such as negative excess volume of mixing [14,15] may be related to the above picture. The degree of the filling into the interstices probably has some distributions. Such environmental difference around the phenyl groups

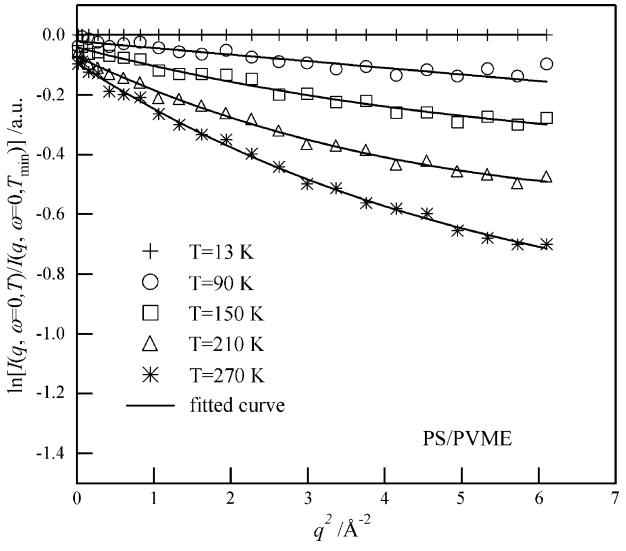

Fig. 5. Logarithm of scattering intensity divided by that at the lowest temperature against q^2 for PS/PVME blend at various temperatures. The solid lines represent the curves fitted with Eq. (9).

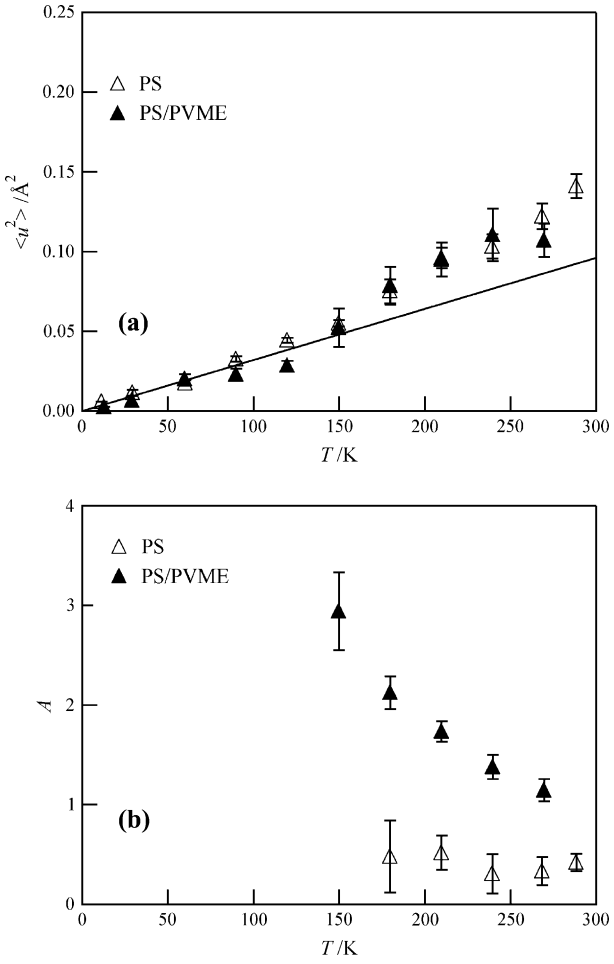

Fig. 6. Temperature dependence of $\langle u^2\rangle_T$ and A_T for pure PS and PS component in PS/PVME blend.

seems to be the main cause of the increase of the dynamical heterogeneity for the PS component in this blend.

4. Conclusion

We investigated the local dynamics of PS/PVME blend by incoherent neutron scattering measurements at $\omega \approx 0$ with a cold triple-axis spectroscopy. Debye–Waller analysis showed the non-Gaussian behavior above a given temperature. The non-Gaussian behavior for the PVME component was found to be caused by broadening of quasielastic scattering arising from rotational motions of methyl groups around $O-CH_3$. On the other hand, blending of PS with PVME leads to a drastic increase in dynamical heterogeneity of the PS component originated from different local environments.

Acknowledgement

The authors greatly appreciate Dr. Metoki for his help on neutron scattering measurements. This work was supported in part by a Grant-in-Aid from Japan Society for the Promotion of Science (16750182).

References

[1] Bee M. Quasielastic neutron scattering: principles and applications in solid state chemistry, biology and material science. Bristol: Adam Hilger; 1988.
[2] Grapengeter HH, Alefeld B, Kosfeld R. Colloid Polym Sci 1987;265: 226.
[3] Hohlweg G, Holzer B, Petry W, Strobl G, Stühn B. Macromolecules 1992;25:6248.
[4] Frick B, Fetters LG. Macromolecules 1994;27:974.
[5] e.g. Kanaya T, Kawaguchi T, Kaji K. J Chem Phys 1996;104:3841.
[6] Kanaya T, Tsukushi I, Kaji K. Prog Theor Phys Suppl 1997;126:133.
[7] Rahman A, Singwi KS, Sjölander A. Phys Rev 1962;126:986.
[8] Zorn R. Phys Rev B 1997;55:6249.
[9] Chahid A, Alegria A, Colmenero J. Macromolecules 1994;27:3282.
[10] Mukhopadhyay R, Alegria A, Colmenero J, Frick B. J Non-Cryst Solids 1998;235–237:233.
[11] Arrighi V, Higgins JS, Burgess AN, Howells WS. Macromolecules 1995; 28:4622.
[12] Takeno H, Koizumi S, Hasegawa H, Hashimoto T. Macromolecules 1996;29:2440.
[13] Fisher EW, Hellmann GP, Spies HW, Hörth FJ, Ecarius U, Wehrle M. Makromol Chem Suppl 1985;12:189.
[14] Shiomi T, Hamada F, Nasako T, Yoneda K, Imai K, Nakajima A. Macromolecules 1990;23:229.
[15] Tsujita Y, Kato M, Kinoshita T, Takizawa A. Polymer 1992;33:773.